

Observation of Rapid Evolution of Convoy Electron Angular Distributions

J. P. Gibbons,⁽¹⁾ S. B. Elston,⁽¹⁾ K. Kimura,^{(1),(a)} R. DeSerio,⁽¹⁾ I. A. Sellin,⁽¹⁾ J. Burgdörfer,⁽¹⁾
J. P. Grandin,⁽²⁾ A. Cassimi,⁽²⁾ X. Husson,^{(2),(b)} L. Liljeby,⁽³⁾ and M. Druetta⁽⁴⁾

⁽¹⁾*Department of Physics, University of Tennessee, Knoxville, Tennessee 37996-1200
and Oak Ridge National Laboratory, Oak Ridge, Tennessee 37831-6377*

⁽²⁾*Centre Interdisciplinaire de Recherche avec les Ions Lourds, Grand Accélérateur National d'Ions Lourds,
BP 5133, 14040 Caen CEDEX, France*

⁽³⁾*Manne Siegbahn Institute of Physics, S-10405 Stockholm, Sweden*

⁽⁴⁾*Laboratoire Traitement du Signal et Instrumentation, Université de St.-Etienne, 42023 St.-Etienne, France*
(Received 29 January 1991)

We present results of doubly differential cross-section measurements for production of convoy electrons from 36-MeV/u Ar ions in thin amorphous carbon targets. Comparison of convoy emission distributions as a function of target thickness reveals rapid evolution of component multipole strengths. Thin-target results are compared with binary ion-atom electron-loss-to-the-continuum predictions. A quantitative model of the multipole evolution bridging the transition from the single- to the plural-collision regime is presented which demonstrates significant competition between one-step and multistep production mechanisms.

PACS numbers: 79.20.Nc, 34.50.Fa

When a projectile of velocity v_p traverses a thin solid target, a cusp-shaped peak in the velocity spectrum of ejected electrons occurs at an electron velocity $v_e = v_p$. These so-called convoy electrons populate low-lying continuum states of the projectile and therefore provide an excellent probe of threshold and near-threshold collision phenomena. In binary ion-atom collisions a similar peak is observed for electron-loss-to-the-continuum (ELC) and electron-capture-to-the-continuum (ECC) processes where the "cusp" electron comes from either the projectile or target, respectively. Although these processes have been extensively studied [1], a number of marked differences between the emission distributions of cusp and convoy electrons remain unexplained. Up to now it has proved difficult to determine the origin of these differences since "density effects" [2], in which multiple excitation of the projectile may precede ionization, become entangled with electron-transport-related phenomena following ionization [3] in the multiple-collision regime.

To disentangle these effects and to explore the evolution of convoy electron angular distributions from their binary atomic collision origins, we have made the first investigations of the transition from single- to plural-collision conditions for convoy electron formation. As pointed out by Rozet *et al.* [4], single-collision conditions (SCC) are achieved for many projectile capture, loss, excitation, and ionization processes in thin foils of thickness on the order of a few $\mu\text{g}/\text{cm}^2$, provided sufficiently fast projectiles are used. For example, for the 36-MeV/u ($v_p = 37$ a.u.) $\text{Ar}^{15+,17+,18+}$ ions used in the present experiments the mean free paths (MFPs) in amorphous carbon for projectile K - and L -shell excitation are ~ 30000 and ~ 16000 a.u., respectively [5], and those for K - and L -shell capture are substantially longer—all very large compared to the ~ 100 - to ~ 2500 -a.u. foil thicknesses we have used.

We were therefore initially surprised to discover that

despite the very long MFPs for the elementary processes of primordial importance in initial convoy generation, the characteristic length for growth and saturation of multipole moments of the angular distributions of the convoys we observed is only ~ 1000 a.u. Explanation of this finding is a central goal of this paper.

This explanation invokes a quantitative model of the convoy electron production process which attributes our observation of a high rate of change of convoy electron angular distributions with target thickness (and hence with projectile "dwell" time) to strong competition between one-step ELC ionization of an incoming projectile electron and two- (or more) step processes involving excitation prior to the convoy-producing ELC event. As a consequence of this competition, it is much more difficult to achieve SCC in ion-solid collisions for convoy electron production than for other atomic processes. For example, when Ar^{17+} ground-state ions are incident on carbon targets with thicknesses only 2% of the MFP for K -shell excitation, we find that more than 50% of the observed convoy emission arises from projectile excited states. Indeed, even with the high- v_p ions used in our experiment and our thinnest targets (~ 100 a.u.), the analysis to be presented indicates that about 10% of the observed convoy electrons from Ar^{17+} were produced from two or more collisions.

The method by which data have been acquired has been described previously [6], so only a brief explanation is needed here. Beams of 36-MeV/u $\text{Ar}^{15+,17+,18+}$, provided at the LISE facility of the Grand Accélérateur National d'Ions Lourds (GANIL), were directed onto self-supporting carbon foils with nominal thicknesses [7] from 0.5 to 21.4 $\mu\text{g}/\text{cm}^2$. The projectile beam diameter was typically ~ 1.0 mm, and its angular spread was limited to about 0.5° . Electrons emitted within a forward cone of 4° were energy selected by a spherical-sector electrostatic electron spectrometer ($\delta E/E \approx 0.01$) equipped with a position-sensitive detector (PSD) capable of resolving

laboratory-frame polar and azimuthal emission angles (θ, ϕ) [6]. The PSD's output, decoded by a simple radiometric method, along with the spectrometer pass energy completely determine, within the resolution limits, the velocity components of a detected electron. Thus, by scanning the spectrometer deflection field across the cusp and obtaining a (θ, ϕ) image at each pass energy, we measure the entire three-dimensional velocity distribution. For the axially symmetric cases of interest here, the three-dimensional distribution is reduced to a two-dimensional one by integrating over the azimuthal slice for which analyzer aberrations are minimal.

Figures 1(a)–1(d) display sample distributions from Ar^{17+} and Ar^{15+} ions on foils of different thicknesses. We have plotted contours of the two-dimensional emission distributions scaled such that isotropic emission would give rise to nearly circular contours. In both cases, the strong transverse emission from the thicker targets is in accord with previous measurements of convoy electron emission under multiple-collision conditions [8]. In particular, the target-thickness transition for Li-like Ar^{15+} , where events are dominated by ELC from the loosely

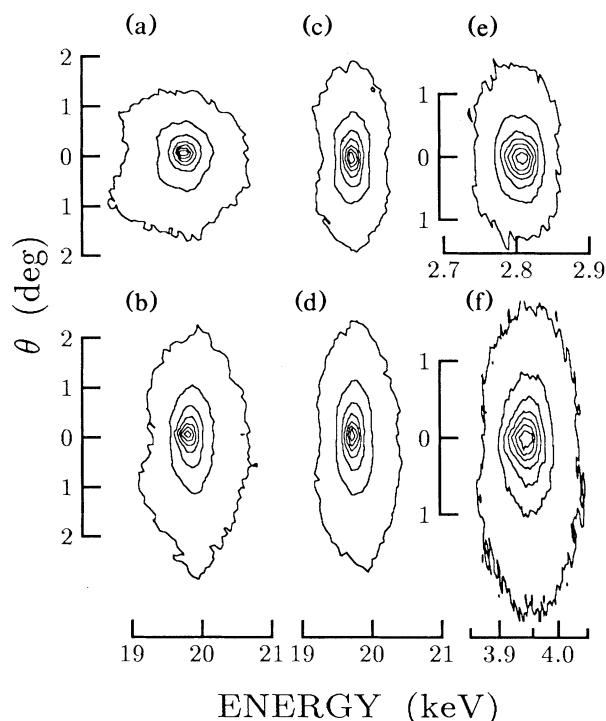


FIG. 1. Contour plots for Ar^{17+} and Ar^{15+} in C ($v=37$ a.u.), and O^{5+} in Ar ($v=14.3$ a.u.) and in $0.5 \mu\text{g}/\text{cm}^2$ C ($v=17$ a.u.). Contours represent multiples of 12.5% of peak height. The horizontal scale indicates laboratory-frame electron energy; the vertical scale indicates electron ejection angle. Isotropic projectile-frame emission would produce nearly circular contours. (a) $\text{Ar}^{17+} + 1.0 \mu\text{g}/\text{cm}^2$ C. (b) $\text{Ar}^{17+} + 21.4 \mu\text{g}/\text{cm}^2$ C. (c) $\text{Ar}^{15+} + 0.5 \mu\text{g}/\text{cm}^2$ C. (d) $\text{Ar}^{15+} + 21.4 \mu\text{g}/\text{cm}^2$ C. (e) $\text{O}^{5+} + \text{Ar}$. (f) $\text{O}^{5+} + 0.5 \mu\text{g}/\text{cm}^2$ C.

bound $n=2$ level, agrees quite well with observed differences between ion-atom and ion-solid spectra for incident Li-like O^{5+} [Figs. 1(e) and 1(f)].

It is convenient to discuss our data quantitatively within a framework established for fast binary collisions which utilizes an expansion for the doubly differential cross section [9],

$$\frac{d\sigma}{d\mathbf{v}'_e} = \frac{\sigma_0}{v'_e} \sum_{k=0}^{\infty} \beta_k P_k(\cos\theta') \quad (\beta_0 \equiv 1), \quad (1)$$

where $\mathbf{v}'_e = \mathbf{v}_e - \mathbf{v}_p$ is the projectile-frame electron velocity and θ' is the polar angle of projectile-frame emission. Extraction of multipole moments β_k has been described previously [6] and is made utilizing a nonlinear least-squares-fitting routine to compare Eq. (1), transformed relativistically to the laboratory frame and convoluted with experimental resolution parameters, to the experimental data in the velocity region $v'_e < 1$ a.u. The inclusion of higher-order v'_e corrections [9] to β_k had no significant effect on the determined multipole moments within quoted error bars.

Evolution of multipole content is shown in Fig. 2, where we have plotted fitted values of the first two asymmetry coefficients, β_1 and β_2 , versus thickness x for all three incident charge states. The presence of a strong di-

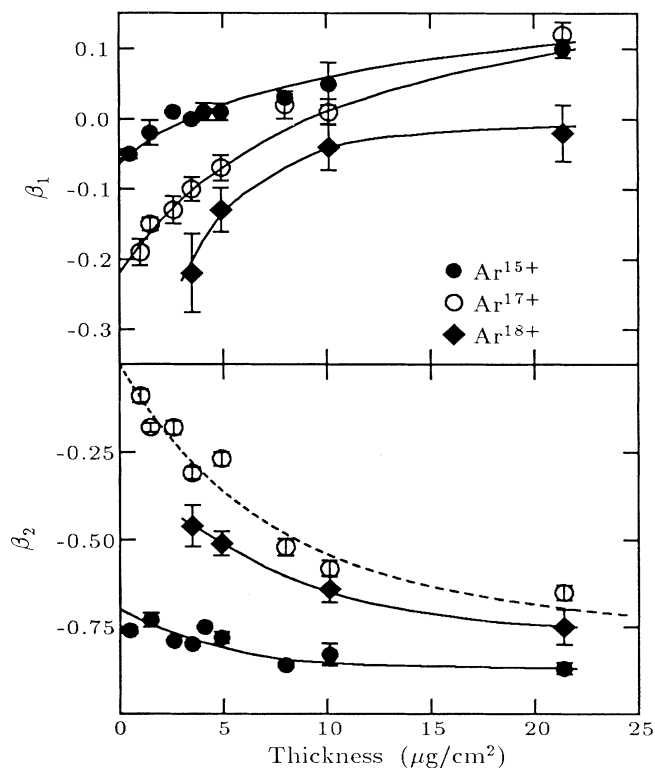


FIG. 2. Extracted anisotropy parameters β_1, β_2 . Solid lines are drawn to guide the eye. The dashed line represents a model described in the text.

pole moment for Ar^{17+} incident on thin foils disagrees with the first-Born-approximation prediction that ELC events produce only even-order moments β_k up to order $k=2n$, where n is the principal quantum number of the initial state from which the electron is lost [10]. It is improbable that ECC events could have produced this behavior in our data: Experimentally determined convoy electron yields from incident Ar^{17+} ions are ~ 50 times the corresponding yields from Ar^{18+} —hence we conclude that ECC can contribute no more than 2% to the Ar^{17+} distributions. These data may indicate that the first Born approximation, which requires that the projectile velocity be much greater than the orbital velocity v' of the initial state, becomes inadequate in describing ELC from the Ar K shell at these velocities ($v_p/v' \approx 2$). There is qualitative agreement between the observed dipole moment and the results of the second-Born-approximation calculation of Jakubassa-Amundsen [11], who finds a negative dipole moment in the case of $\text{He}^+ + \text{He}$ with projectile velocities $v_p \lesssim 4v'$.

Variations in the magnitude of the quadrupole term, β_2 , are larger for incident Ar^{17+} than for Ar^{15+} . This is thought to indicate a larger variation in β_2 between emission from $n=1$ and $n=2$ levels than between emission from $n=2$ and higher levels. The Ar^{15+} data show a small change from approximately -0.70 to -0.85 ; the initial value agrees with predictions of ion-atom ELC β_2 from $n=2$ [10,12], while the final value agrees with the more transverse distributions observed in ion-solid collisions at lower velocities [8].

As seen in Fig. 2, the coefficients β_1 and β_2 change rapidly and have nearly equilibrated in our thicker targets. We attribute this to growth in convoy electron production from excited states, and have developed a model of the β_k evolution incorporating both ground- and excited-state contributions to test this hypothesis. Since $\beta_k(x)$ represents multipole contributions from different initial states, we write

$$\beta_k(x) = \frac{\sum_i \beta_k^i Y^i(x)}{\sum_i Y^i(x)}, \quad (2)$$

where the summation is made over the ground ($i=1$) and all contributing excited states ($i>1$). β_k^i is the multipole moment associated with emission from state i ; $Y^i(x)$ is the yield of convoy electrons emitted from state i into the velocity region of the fit ($v_e' < 1$ a.u.). Thus the denominator of Eq. (2) represents the total yield of convoy electrons [13].

We focus here on the quadrupole moment β_2 for incident Ar^{17+} ($1s$), since it has the largest relative change in magnitude. The evolution of the other multipoles can be analyzed under similar lines, but this provides no additional insight to the rapid multipole equilibration. Since the evolution of β_2 for Ar^{15+} ($1s^2 2s$) is weak, we assume that the quadrupole moments of ELC from excited states of $n \geq 2$ are approximately equal (≈ -0.85). We use the measured Ar^{17+} β_2 for the thinnest targets (≈ 0.0)

for the ground-state β_2^1 .

This analysis uses previous expressions [14] for the ground-state and excited-state yields which, for targets much thinner than the convoy electron attenuation length [15] (where the majority of the multipole evolution takes place [16]), may be written

$$Y^1(x) = n_T \sigma_1^{\text{ELC}} x \equiv ax, \quad (3)$$

$$Y^{i>1}(x) = \sum_{i>1} \frac{1}{2} n_T^2 \sigma_i^{\text{ELC}} x^2 \equiv bx^2,$$

where n_T is the target density. σ_i^1 represents the cross section for excitation from the $n=1$ to state i and σ_i^{ELC} is the cross section for ELC from state i . For these cross sections we have used available theoretical values [5,12] appropriate for $v_p = 36$ a.u. $\text{Ar}^{17+} + \text{C}$. The products of excitation and ELC cross sections for different excited states indicate that a broad range of n (≤ 10) contributes significantly to the total yield. For large n , ELC cross sections approach an asymptotic limit [17] while excitation cross sections fall $\propto n^{-3}$. As a result, states with $n > 10$ contribute less than 10% to the total yield.

The difference in the thickness dependences of the single-collision yield $Y^1(x)$ and the plural-collision (two-step) yield $Y^{i>1}(x)$ leads to multipole evolution; the ratio of amplitudes, b/a , determines the evolution rate $d\beta_2/dx$. There are two features which cause the observed rapid evolution rate. First, both amplitudes are directly propor-

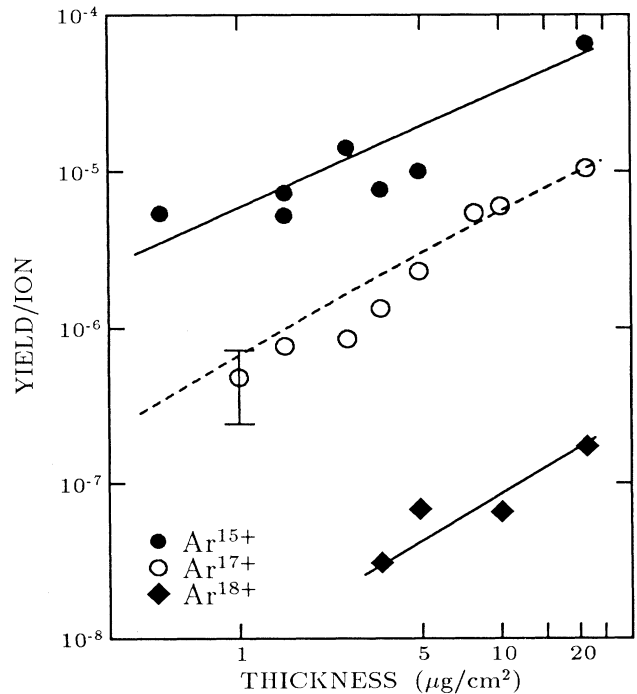


FIG. 3. Experimental yields of convoy electrons vs target thickness. Solid lines are drawn to guide the eye. The dashed line represents a model of the Ar^{17+} yield (see text).

tional to the ELC cross section from their respective states which is strongly enhanced for excited states. For example, the ratio of the ELC cross section from $n=2$ to that from $n=1$, determined by comparing our experimental convoy yields from Ar^{15+} and Ar^{17+} in thin foils, is about 15, in agreement with recent theoretical calculations [12]. Second, the contribution from many excited states ($n > 2$) further increases the evolution rate. In this collision system, the total excited-state contribution is about 10 times that due to $n=2$ alone.

The resulting $\beta_2(x)$ (the dashed curve in Fig. 2) reproduces the data remarkably well. We emphasize here that no free parameters and only atomic cross sections were used to obtain this agreement. Furthermore, using an estimate for the PSD efficiency of about 40% [18], the total convoy yield compares well with the experimental convoy yield from Ar^{17+} as shown in Fig. 3.

In conclusion, while the thinnest-target data are consistent with a binary ion-atom description, modeling of the rapid convoy emission evolution requires enhanced two-step convoy production from excited states, despite long characteristic lengths for excitation. Both the observed rapid evolution rate and the presence of high-ordered multipoles provide clear-cut evidence for the population of high- n projectile excited states in the bulk—even when the orbital size exceeds mean interatomic spacings. The need to incorporate single- and multiple-collision effects simultaneously to account for convoy angular distributions illustrates a corresponding need for great care in distinguishing single- from multiple-collision criteria in solid targets, even at very high v_p .

The authors are grateful to the technical staff of GANIL for providing a high-quality argon beam. This work was supported by the National Science Foundation and by the U.S. Department of Energy under Contract No. DE-AC05-84OR21400 with Martin Marietta Energy Systems, Inc.

^(a)On leave from Department of Engineering Science, Kyoto

University, Kyoto, Japan.

^(b)Permanent address: Laboratoire de Spectroscopie Atomique, ISMRA, 14050 Caen CEDEX, France.

- [1] *Forward Electron Ejection in Ion Collisions*, edited by K. O. Groeneveld *et al.* (Springer, Berlin, 1984); M. W. Lucas and W. Steckelmacher, in *High Energy Ion-Atom Collisions*, edited by D. Berényi and G. Hock (Springer, Berlin, 1988), p. 229; M. Breinig *et al.*, Phys. Rev. A **25**, 3015 (1982).
- [2] N. Bohr and J. Lindhard, K. Dan. Vidensk. Selsk. Mat. Fys. Medd. **28**, No. 7 (1954).
- [3] J. Burgdörfer and J. P. Gibbons, Phys. Rev. A **42**, 1206 (1990).
- [4] J. P. Rozet *et al.*, Phys. Rev. Lett. **58**, 337 (1987).
- [5] G. Gillespie, Phys. Rev. A **18**, 1967 (1978); **22**, 454 (1980). Our studies of charge-state evolution for incident Ar^{15+} are in harmony with the large mean free paths quoted.
- [6] S. B. Elston, Nucl. Instrum. Methods Phys. Res., Sect. B **24/25**, 214 (1987).
- [7] The absolute values of foil thicknesses given by the supplier (Arizona Foil Co.) are used.
- [8] S. D. Berry *et al.*, J. Phys. B **19**, L149 (1985).
- [9] W. Meckbach, I. B. Nemirovsky, and C. Garibotti, Phys. Rev. A **24**, 1793 (1981).
- [10] J. Burgdörfer *et al.*, Phys. Rev. A **28**, 3227 (1983); **33**, 1578 (1986).
- [11] D. H. Jakubassa-Amundsen, J. Phys. B **23**, 3335 (1990).
- [12] G. Szabo (private communication).
- [13] H. D. Betz *et al.*, Nucl. Instrum. Methods Phys. Res., Sect. B **33**, 185 (1988).
- [14] W. Meckbach and P. Focke, Nucl. Instrum. Methods Phys. Res., Sect. B **33**, 255 (1988); H.-P. Hülskötter *et al.*, Nucl. Instrum. Methods Phys. Res., Sect. B **24/25**, 147 (1987).
- [15] J. Ashley *et al.*, Thin Solid Films **60**, 361 (1979).
- [16] We note that the deviation in $\beta_2(x)$ due to the approximations of Eqs. (3) are $< 3\%$ for the thickness range of this experiment ($\lesssim 25 \mu\text{g}/\text{cm}^2$).
- [17] D. Rösenthaler *et al.*, J. Phys. B **16**, L233 (1983).
- [18] M. Galanti *et al.*, Rev. Sci. Instrum. **42**, 1818 (1971); R. S. Gao *et al.*, *ibid.* **55**, 1756 (1984).